Perspectives of Core-Collapse Supernovae beyond SN 1987A

H.-Th. Janka and W. Keil

Max-Planck-Institut für Astrophysik, Karl-Schwarzschild-Str. 1, D-85740 Garching, Germany

Abstract. The observation of neutrinos from Supernova 1987A has confirmed the theoretical conjecture that these particles play a crucial role during the collapse of the core of a massive star. Only one per cent of the energy they carry away from the newly formed neutron star may account for all the kinetic and electromagnetic energy responsible for the spectacular display of the supernova explosion. However, the neutrinos emitted from the collapsed stellar core at the center of the explosion couple so weakly to the surrounding matter that convective processes behind the supernova shock and/or inside the nascent neutron star might be required to increase the efficiency of the energy transfer to the stellar mantle and envelope. The conditions for a successful explosion by the neutrino-heating mechanism and the possible importance of convection in and around the neutron star are shortly discussed. Neutrino-driven explosions turn out to be very sensitive to the parameters describing the neutrino emission of the proto-neutron star and to the details of the dynamical processes in the collapsed stellar core. Therefore uniform explosions with a well defined energy seem unlikely and type-II supernova explosions do not offer promising perspectives for being useful as standard candles.

1. Introduction

Even after ten exciting years SN 1987A keeps rapidly evolving and develops new, unexpected sides like an aging character. In the first few months the historical detection of 24 neutrinos in the underground facilities of the Kamiokande, IMB, and Baksan laboratories caused hectic activity among scientists from very different fields. In the subsequent years the scene was dominated by the rise and slow decay of light emission in all wavelengths which followed the outbreak of the supernova shock and contained a flood of data about the structure of the progenitor star and the dynamics of the explosion. Now that the direct emission has settled down to a rather low level, the supernova light which is reflected from circumstellar structures provides insight into the progenitor's evolution. Even more information about the latter can be expected when the supernova shock hits the inner ring in a few years.

The neutrino detections in connection with SN 1987A were the final proof that neutrinos take up the bulk of the energy during stellar core collapse and neutron star formation. Lightcurve and spectra of SN 1987A bear clear evidence
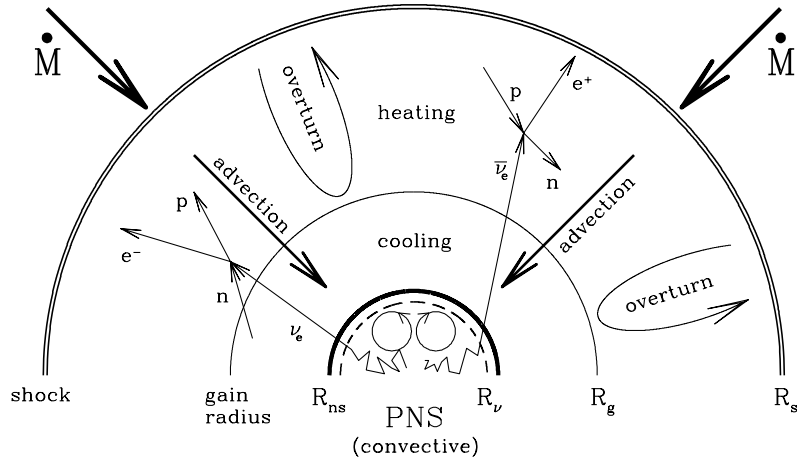
Figure 1. Sketch of the post-collapse stellar core during the neutrino heating and shock revival phase. At the center, the neutrino emitting proto-neutron star (PNS) with radius R_{ns} is shown. The average radius where neutrinos decouple from the matter of the nascent neutron star and stream off essentially freely ("neutrinosphere") is denoted by R_ν. The neutrino cooling layer and the neutrino heating region behind the supernova shock (at R_{s}) are separated by the "gain radius" R_{g}. Matter is accreted into the shock at a rate $\dot{M}$ and is partly advected through the gain radius into the cooling region and onto the neutron star. Convective overturn between the gain radius and the shock increases the efficiency of neutrino heating. Convective activity inside the proto-neutron star raises the neutrino luminosities and thus amplifies the neutrino energy deposition.

of large-scale mixing in the stellar mantle and envelope and of fast moving Ni clumps. Both might indicate that macroscopic anisotropies and inhomogeneities were already present near the formation region of Fe group elements during the very early stages of the explosion. Spherically symmetric models had been suggesting for some time already that regions inside the newly formed neutron star and in the neutrino-heated layer around it might be convectively unstable. These theoretical results and the observational findings in SN 1987A were motivation to study stellar core collapse and supernova explosions with multi-dimensional simulations.

In this article convective overturn in the neutrino-heated region around the collapsed stellar core is discussed concerning its effects on the neutrino energy deposition and its potential importance for the revival of the stalled bounce shock and thus for triggering the supernova explosion. Convective activity inside the proto-neutron star is suggested as a possibly crucial boost of the neutrino luminosities on a timescale of a few hundred milliseconds after core bounce. The first two-dimensional simulations that follow the evolution of the nascent neutron star for more than one second are shortly described.

2. Neutrino-driven explosions and convective overturn

2.1. Neutrino heating and supernova explosions

Figure 1 displays a sketch of the neutrino cooling and heating regions outside the proto-neutron star at the center. The main processes of neutrino energy deposition are the charged-current reactions $\nu_e + n \to p + e^-$ and $\bar{\nu}_e + p \to n + e^+$ (Bethe & Wilson 1985). The heating rate per nucleon (N) is approximately

$$Q_\nu^+ \approx 110 \cdot \frac{L_{\nu,52}\langle\epsilon_{\nu,15}^2\rangle}{r_7^2 \, f} \cdot \left\{ \begin{matrix} Y_n \\ Y_p \end{matrix} \right\} \quad \left[\frac{\text{MeV}}{\text{s} \cdot N} \right] \, , \tag{1}$$

where Y_n and Y_p are the number fractions of free neutrons and protons, respectively, $L_{\nu,52}$ denotes the luminosity of ν_e or $\bar{\nu}_e$ in 10^{52} erg/s, r_7 the radial position in 10^7 cm, and $\langle\epsilon_{\nu,15}^2\rangle$ the average of the squared neutrino energy measured in units of $15\,\text{MeV}$. f is the angular dilution factor of the neutrino radiation field (the "flux factor", which is equal to the mean value of the cosine of the angle of neutrino propagation relative to the radial direction) which varies between about 0.25 at the neutrinosphere and 1 for radially streaming neutrinos far out. Using this energy deposition rate, neglecting loss due to re-emission of neutrinos, and assuming that the gravitational binding energy of a nucleon in the neutron star potential is (roughly) balanced by the sum of internal and nuclear recombination energies after accretion of the infalling matter through the shock, one can estimate the explosion energy to be of the order

$$E_{\text{exp}} \approx 2.2 \cdot 10^{51} \cdot \frac{L_{\nu,52}\langle\epsilon_{\nu,15}^2\rangle}{r_7^2 \, f} \left(\frac{\Delta M}{0.1 \, M_\odot} \right) \left(\frac{\Delta t}{0.1\,\text{s}} \right) - E_{\text{gb}} + E_{\text{nuc}} \quad [\text{erg}] \, . \tag{2}$$

ΔM is the heated mass, Δt the typical heating timescale, E_{gb} the (net) total gravitational binding energy of the overlying, outward accelerated stellar layers, and E_{nuc} the additional energy from explosive nucleosynthesis which is typically a few 10^{50} erg and roughly compensates E_{gb} for progenitors with main sequence masses of less than about $20\,M_\odot$. Since the gain radius, shock radius, and Δt and thus also ΔM depend on $L_\nu\langle\epsilon_\nu^2\rangle$, the sensitivity of E_{exp} to the neutrino emission parameters is even stronger than suggested by Eq. (2).

2.2. Convective overturn in the neutrino-heated region

Convective instabilities in the layers adjacent to the nascent neutron star are a natural consequence of the negative entropy gradient built up by neutrino heating (Bethe 1990) and are seen in recent two- and three-dimensional simulations (Burrows et al. 1995; Herant et al. 1992, 1994; Janka & Müller 1995, 1996; Mezzacappa et al. 1997; Miller et al. 1993; Shimizu et al. 1994). Figure 2 shows the entropy distribution between proto-neutron star and supernova shock about 170 ms after core bounce for one of the calculations by Janka & Müller (1996). Although there is general agreement about the existence of this unstable region between the radius of maximum neutrino heating (which is very close outside the "gain radius" R_{g}, i.e. the radius where neutrino cooling switches into net heating) and the shock position R_{s}, the strength of the convective overturn and its importance for the success of the neutrino-heating mechanism in driving the explosion of the star is still a matter of vivid debate.
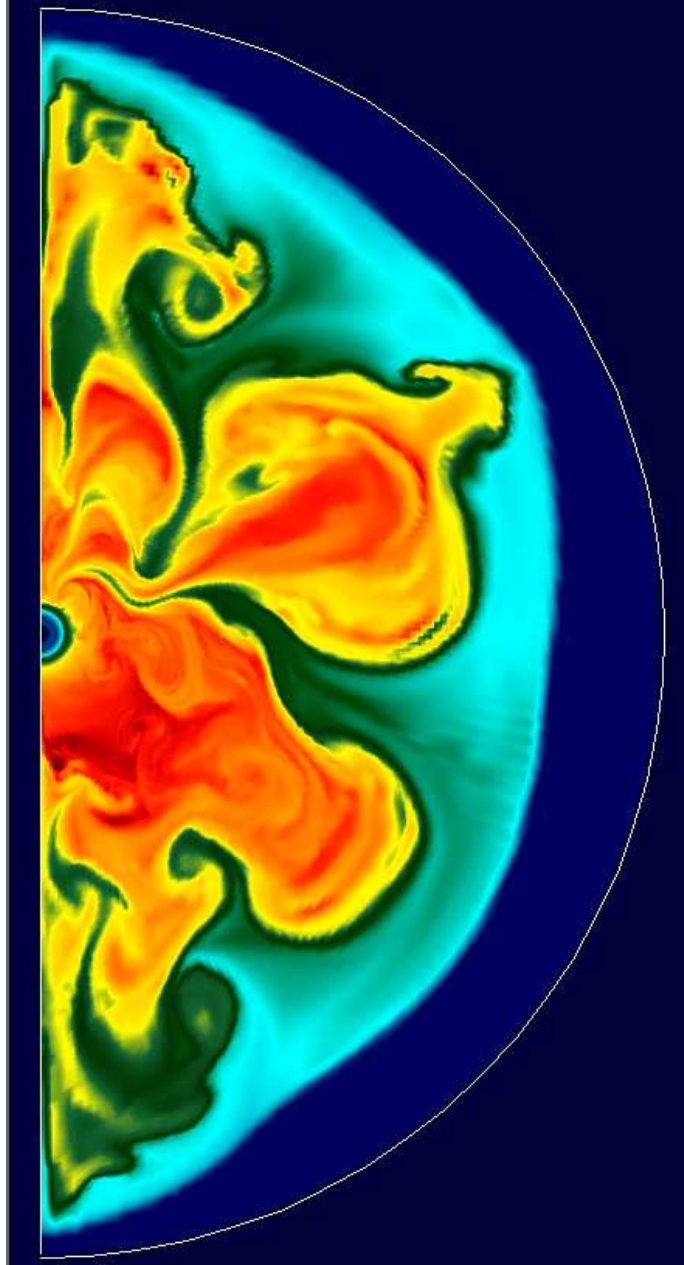
Figure 2.   Inhomogeneous distribution of cool and hot gas between the nascent neutron star (left side, middle) and the supernova shock front (bumpy, hemispheric discontinuity) during the first second of the explosion. Neutrino-heated matter rises and expands in mushroom-like bubbles, while cool gas flows down toward the neutron star in narrow streams. The radius of the semicircle is 1600 km, the shock is at about 1400 km.
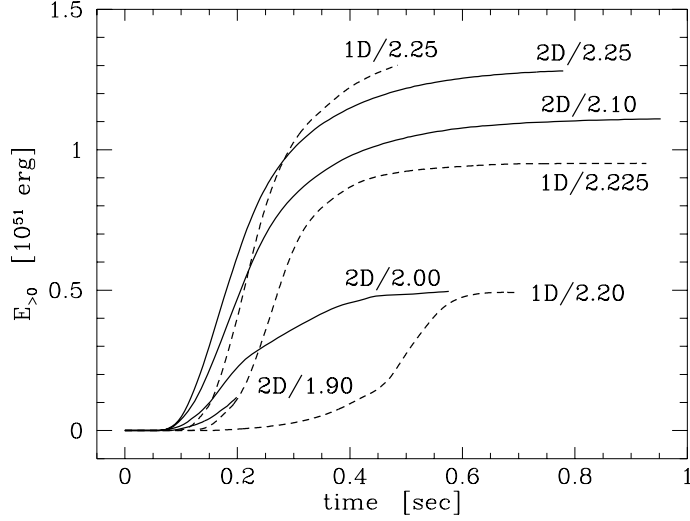
Figure 3.   Explosion energies $E_{>0}(t)$ for 1D (dashed) and 2D (solid) simulations with different assumed ν_e and $\bar\nu_e$ luminosities (labels give values in 10^{52} erg/s) from the proto-neutron star. Below the smallest given luminosities the considered $15\,M_\odot$ star does not explode in 1D and acquires too low an expansion energy in 2D to unbind the stellar mantle and envelope. $E_{>0}$ is defined to include the sum of internal, kinetic, and and gravitational energy for all zones where this sum is positive (the gravitational binding energies of stellar mantle and envelope and additional energy release from nuclear burning are not taken into account).

The effect of convective overturn in the neutrino-heated region on the shock is two-fold. On the one hand, heated matter from the region close to the gain radius rises outward and at the same time is replaced by cool gas flowing down from the postshock region. Since the production reactions of neutrinos ($e^\pm$ capture on nucleons and thermal processes) are very temperature sensitive, the expansion and cooling of rising plasma reduces the energy loss by reemission of neutrinos. Moreover, the net energy deposition by neutrinos is enhanced as more cool material is exposed to the large neutrino fluxes just outside the gain radius where the neutrino heating rate peaks (the radial dilution of the fluxes roughly goes as $1/r^2$). On the other hand, hot matter floats into the postshock region and increases the pressure there. Thus the shock is pushed further out which leads to a growth of the gain region and therefore also of the net energy transfer from neutrinos to the stellar gas.

2.3.   Requirements for neutrino-driven explosions

In order to get explosions by the delayed neutrino-heating mechanism, certain conditions need to be fulfilled. Expansion of the postshock region requires sufficiently large pressure gradients near the radius R_{cut} of the developing mass cut. If one neglects self-gravity of the gas in this region and assumes the density pro-

file to be a power law, $\rho(r) \propto r^{-n}$ (which is well justified according to numerical simulations which yield a power law index of $n \approx 3$; see also Bethe 1993), one gets $P(r) \propto r^{-n-1}$ for the pressure in an atmosphere near hydrostatic equilibrium, and outward acceleration is maintained as long as the following condition for the "critical" internal energy density ε holds:

$$\left. \frac{\varepsilon_{\mathrm{c}}}{GM\rho/r} \right|_{R_{\mathrm{cut}}} > \frac{1}{(n+1)(\gamma-1)} \cong \frac{3}{4} , \qquad (3)$$

where use was made of the relation $P = (\gamma - 1)\varepsilon$. The numerical value was obtained for $\gamma = 4/3$ and $n = 3$. This condition can be converted into a criterion for the entropy per baryon, s. Using the thermodynamical relation for the entropy density normalized to the baryon density n_b, $s = (\varepsilon+P)/(n_b T)-\sum_i \eta_i Y_i$ where η_i ($i = n$, p, e^-, e^+) are the particle chemical potentials divided by the temperature, and assuming completely disintegrated nuclei behind the shock so that the number fractions of free protons and neutrons are $Y_p = Y_e$ and $Y_n = 1 - Y_e$, respectively, one gets

$$s_{\mathrm{c}}(R_{\mathrm{cut}}) \gtrsim \left. 15 \frac{M_{1.1}}{r_7 T} \right|_{R_{\mathrm{cut}}} - \left. \ln \left(1.27 \cdot 10^{-3} \frac{\rho_9 Y_n}{T^{3/2}} \right) \right|_{R_{\mathrm{cut}}} \quad [k_{\mathrm{B}}/N] . \qquad (4)$$

In this approximate expression a term with a factor Y_e was dropped (its absolute value being usually less than 0.5 in the considered region), nucleons are assumed to obey Boltzmann statistics, and, normalized to representative values, $M_{1.1}$ is measured in units of $1.1\,M_\odot$, ρ_9 in $10^9\,\mathrm{g/cm}^3$, and r_7 in $10^7\,\mathrm{cm}$. Inserting typical numbers ($T \approx 1.5\,\mathrm{MeV}$, $Y_n \approx 0.3$, $R_{\mathrm{cut}} \approx 1.5 \cdot 10^7\,\mathrm{cm}$), one obtains $s > 15\,k_{\mathrm{B}}/N$, which gives an estimate of the entropy in the heating region when the star is going to explode.

These requirements can be coupled to the neutrino emission of the proto-neutron star by the following considerations. A stalled shock is converted into a moving one only when the neutrino heating is strong enough to increase the pressure behind the shock by a sufficient amount. Considering the Rankine-Hugoniot relations at the shock, Bruenn (1993) derived a criterion for the heating rate per unit mass, q_ν, behind the shock that guarantees a positive postshock velocity ($u_1 > 0$):

$$q_\nu > \frac{2\beta - 1}{\beta^3(\beta-1)(\gamma-1)} \frac{|u_0|^3}{\eta R_{\mathrm{s}}} . \qquad (5)$$

Here β is the ratio of postshock to preshock density, $\beta = \rho_1/\rho_0$, γ the adiabatic index of the gas (assumed to be the same in front and behind the shock), and η defines the fraction of the shock radius R_{s} where net heating by neutrino processes occurs: $\eta = (R_{\mathrm{s}} - R_{\mathrm{g}})/R_{\mathrm{s}}$. u_0 is the preshock velocity, which is a fraction α (analytical and numerical calculations show that typically $\alpha \approx 1/\sqrt{2}$) of the free fall velocity, $u_0 = \alpha\sqrt{2GM/r}$. Assuming a strong shock, one has $\beta = (\gamma + 1)/(\gamma - 1)$ which becomes $\beta = 7$ for $\gamma = 4/3$. With numbers typical of the collapsed core of the $15\,M_\odot$ star considered by Janka & Müller (1996), $R_{\mathrm{s}} = 200\,\mathrm{km}$, $\eta \approx 0.4$, and an interior mass $M = 1.1\,M_\odot$, one finds for the threshold luminosities of ν_e and $\bar\nu_e$:

$$L_{\nu,52}\langle \epsilon_{\nu,15}^2 \rangle > 2.0 \frac{M_{1.1}^{3/2}}{R_{\mathrm{s},200}^{1/2}} . \qquad (6)$$

6

The existence of such a threshold luminosity of the order of $2 \cdot 10^{52}$ erg/s is underlined by Fig. 3 where the explosion energy $E_{>0}$ as function of time is shown for numerical calculations of the same post-collapse model but with different assumed neutrino luminosities from the proto-neutron star. $E_{>0}$ is defined to include the sum of internal, kinetic, and gravitational energy for all zones where this sum is positive (the gravitational binding energies of stellar mantle and envelope and additional energy release from nuclear burning are not taken into account). For one-dimensional simulations with luminosities below $1.9 \cdot 10^{52}$ erg/s we could not get explosions when the proto-neutron star was assumed static, and the threshold for the ν_e and $\bar{\nu}_e$ luminosities was $2.2 \cdot 10^{52}$ erg/s when the neutron star was contracting (see Janka & Müller 1996). The supporting effects of convective overturn between the gain radius and the shock described in Sect. 2.2. lead to explosions even below the threshold luminosities for the spherically symmetric case, to higher values of the explosion energy for the same neutrino luminosities, and to a faster development of the explosion. This can clearly be seen by comparing the solid (2D) and dashed (1D) lines in Fig. 3.

The results of Fig. 3 also show that the explosion energy is extremely sensitive to the neutrino luminosities and mean energies. This holds in 1D as well as in 2D. The question can be asked why neutrino-driven explosions should be self-regulated. Which kind of feedback should prevent the explosion from being more energetic than a few times 10^{51} erg? Certainly, the neutrino luminosities in current models can hardly power an explosion and therefore a way to overpower it is not easy to imagine. Nevertheless, Fig. 3 and Eq. (2) offer an answer to the question: When the matter in the neutrino-heated region outside the gain radius has absorbed roughly its gravitational binding energy from the neutrino fluxes, it starts to expand outward (see Eq. (3)) and moves away from the region of strongest heating. Since the onset of the explosion shuts off the re-supply of the heating region with cool gas, the curves in Fig. 3 approach a saturation level as soon as the expansion gains momentum and the density in the heating region decreases. Thus the explosion energy depends on the strength of the neutrino heating, which scales with the ν_e and $\bar{\nu}_e$ luminosities and mean energies, and it is limited by the amount of matter ΔM in the heating region and by the duration of the heating (see Eq. (2)), both of which decrease when the heating is strong and expansion happens fast.

This also implies that neutrino-driven explosions can be "delayed" (up to a few 100 ms after core bounce) but are *not* "late" (after a few seconds) explosions. The density between the gain radius and the shock decreases with time because the proto-neutron star contracts and the mass infall onto the collapsed core declines steeply with time. Therefore the mass ΔM in the heated region drops rapidly and energetic explosions by the neutrino-heating mechanism become less favored at late times.

Moreover, Fig. 3 tells us that convection is *not necessary* to get an explosion and convective overturn is *no guarantee* for strong explosions. Therefore one must suspect that neutrino-driven type-II explosions should reveal a considerable spread of the explosion energies, even for similar progenitor stars. Rotation in the stellar core, small differences of the core mass or statistical variations in the dynamical events that precede and accompany the explosion may lead to
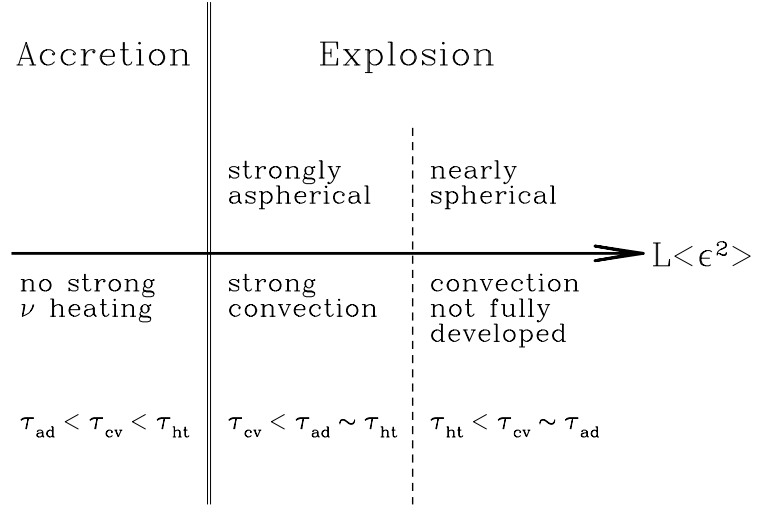
Accretion	Explosion

	strongly aspherical	nearly spherical

$\longrightarrow$ L$<\epsilon^2>$

no strong ν heating	strong convection	convection not fully developed

$\tau_{\mathrm{ad}} < \tau_{\mathrm{cv}} < \tau_{\mathrm{ht}}$	$\tau_{\mathrm{cv}} < \tau_{\mathrm{ad}} \sim \tau_{\mathrm{ht}}$	$\tau_{\mathrm{ht}} < \tau_{\mathrm{cv}} \sim \tau_{\mathrm{ad}}$

Figure 4. Order scheme for the dependence of the post-collapse dynamics on the strength of the neutrino heating as a function of $L_\nu \langle \epsilon_\nu^2 \rangle$. The destiny of the star – accretion or explosion – depends on the relative size of the timescales of neutrino heating, τ_{ht}, matter advection through the gain region onto the proto-neutron star, τ_{adv}, and growth of convective instabilities, τ_{cv}. With a larger value of $L_\nu \langle \epsilon_\nu^2 \rangle$ the heating timescale as well as τ_{cv} decrease, the latter due to a steeper entropy gradient built up by the neutrino energy deposition near the gain radius.

some variability. The potential sensitivity to the properties and structure of the progenitor star, to the dynamical events during and after core collapse, and to the neutrino emission parameters of the proto-neutron star do not make type-II supernovae promising candidates for standard candles with a rather well defined value of the explosion energy.

2.4. When is neutrino-driven convection crucial for an explosion?

The role of convective overturn and its importance for the explosion can be further illuminated by considering the three timescales of neutrino heating, τ_{ht}, advection of accreted matter through the gain radius into the cooling region and onto the neutron star (compare Fig. 1), τ_{ad}, and growth of convective instabilities, τ_{cv}. The evolution of the shock — accretion or explosion — is determined by the relative sizes of these three timescales. Straightforward considerations show that they are of the same order and the destiny of the star is therefore a result of a tight competition between the different processes (see Fig. 4).

The heating timescale is estimated from the initial entropy s_{i}, the critical entropy s_{c} (Eq. (4)), and the heating rate per nucleon (Eq. (1)) as

$$\tau_{\mathrm{ht}} \approx \frac{s_{\mathrm{c}} - s_{\mathrm{i}}}{Q_\nu^+/(k_{\mathrm{B}}T)} \approx 45\,\mathrm{ms} \cdot \frac{s_{\mathrm{c}} - s_{\mathrm{i}}}{5k_{\mathrm{B}}/N} \frac{R_{\mathrm{g},7}^2 (T/2\mathrm{MeV})\,f}{(L_\nu/2 \cdot 10^{52}\mathrm{erg/s})\langle \epsilon_{\nu,15}^2 \rangle} \ . \tag{7}$$

8

With a postshock velocity of $u_1 = u_0/\beta \approx (\gamma-1)\sqrt{GM/R_\mathrm{s}}/(\gamma+1)$ the advection timescale is

$$\tau_\mathrm{ad} \approx \frac{R_\mathrm{s} - R_\mathrm{g}}{u_1} \approx 52\,\mathrm{ms} \cdot \left(1 - \frac{R_\mathrm{g}}{R_\mathrm{s}}\right) \frac{R_\mathrm{s,200}^{3/2}}{\sqrt{M_{1.1}}}\,, \tag{8}$$

where the gain radius can be determined as

$$R_\mathrm{g,7} \cong 0.4 \left(\frac{L_\nu}{2 \cdot 10^{52}\mathrm{erg/s}}\right)^{-1/4} \langle \epsilon_{\nu,15}^2 \rangle^{-1/4} f^{1/4} \left(\frac{R_\mathrm{ns}}{25\mathrm{km}}\right)^{3/2} \tag{9}$$

from the requirement that the heating rate, Eq. (1), is equal to the cooling rate per nucleon, $Q_\nu^- \approx 288(T/2\mathrm{MeV})^6\,\mathrm{MeV}/(N \cdot \mathrm{s})$, when use is made of the power-law behavior of the temperature according to $T(r) \approx 4\,\mathrm{MeV}\,(R_\mathrm{ns}/r)$ with R_ns being the proto-neutron star radius (roughly equal to the neutrinosphere radius). The growth timescale of convective instabilities in the neutrino-heated region depends on the gradients of entropy and lepton number through the growth rate of Ledoux convection, σ_L (g is the gravitational acceleration):

$$\tau_\mathrm{cv} \approx \frac{\ln{(100)}}{\sigma_\mathrm{L}} \approx 4.6 \left\{\frac{g}{\rho}\left[\left(\frac{\partial \rho}{\partial s}\right)_{Y_e,P} \frac{\mathrm{d}s}{\mathrm{d}r} + \left(\frac{\partial \rho}{\partial Y_e}\right)_{s,P} \frac{\mathrm{d}Y_e}{\mathrm{d}r}\right]\right\}^{-1/2} \gtrsim 50\,\mathrm{ms}\,. \tag{10}$$

The numerical value is representative for those obtained in hydrodynamical simulations (e.g., Janka & Müller 1996). τ_cv of Eq. (10) is sensitive to the detailed conditions between neutrinosphere (where Y_e has typically a minimum), gain radius (where s develops a maximum), and the shock. The neutrino heating timescale is shorter for larger values of the neutrino luminosity L_ν and mean squared neutrino energy $\langle \epsilon_\nu^2 \rangle$, while both τ_ht and τ_ad depend strongly on the gain radius, τ_ad also on the shock position.

In order to be a crucial help for the explosion, convective overturn in the neutrino-heated region must start on a sufficiently short timescale. This happens only in a rather narrow window of $L_\nu\langle \epsilon_\nu^2 \rangle$ where $\tau_\mathrm{cv} < \tau_\mathrm{ad} \sim \tau_\mathrm{ht}$ (Fig. 3). For smaller neutrino luminosities the heating is too weak to create a sufficiently large entropy maximum and the convective instability cannot develop before the accreted gas is advected through the gain radius ($\tau_\mathrm{ad} < \tau_\mathrm{cv} < \tau_\mathrm{ht}$). In this case neither with nor without convective processes energetic explosions can occur (see also Sect. 2.3.). For larger neutrino luminosities the neutrino heating is so strong ($\tau_\mathrm{ht} < \tau_\mathrm{cv} \sim \tau_\mathrm{ad}$) that expansion of the postshock layers has set in before the convective activity reaches a significant level.

3. Convection inside the nascent neutron star

Convective energy transport inside the newly formed neutron star can increase the neutrino luminosities considerably (Burrows 1987). This could be crucial for energizing the stalled supernova shock (Mayle & Wilson 1988; Wilson & Mayle 1988, 1993; see also Sect. 2.).

Negative lepton number and entropy gradients have been seen in several one-dimensional (spherically symmetrical) simulations of the neutrino-cooling phase of nascent neutron stars (Burrows & Lattimer 1986; Burrows 1987; Keil
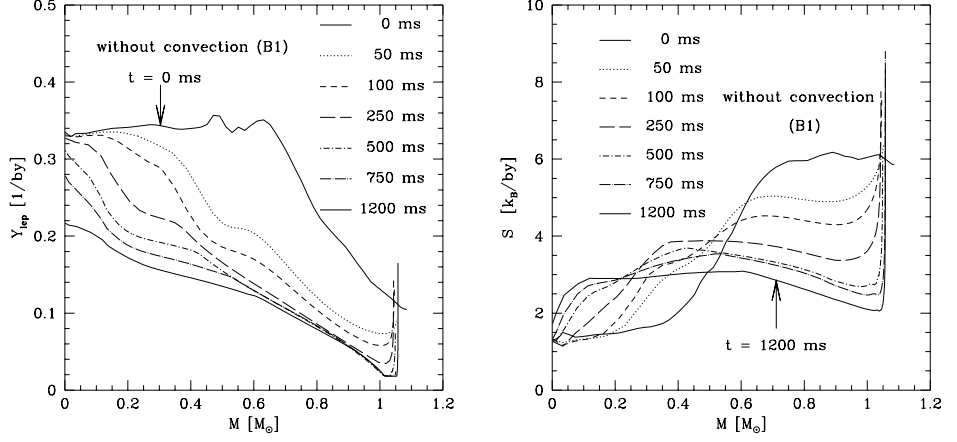
Figure 5. Profiles of the lepton fraction $Y_{\mathrm{lep}} = n_{\mathrm{lep}}/n_b$ (left) and of the entropy per nucleon, s, (right) as functions of enclosed (baryonic) mass for different times in a one-dimensional simulation of the neutrino cooling of a $\sim 1.1\,M_\odot$ proto-neutron star. Negative gradients of lepton number and entropy suggest potentially convectively unstable regions. Time is (roughly) measured from core bounce.
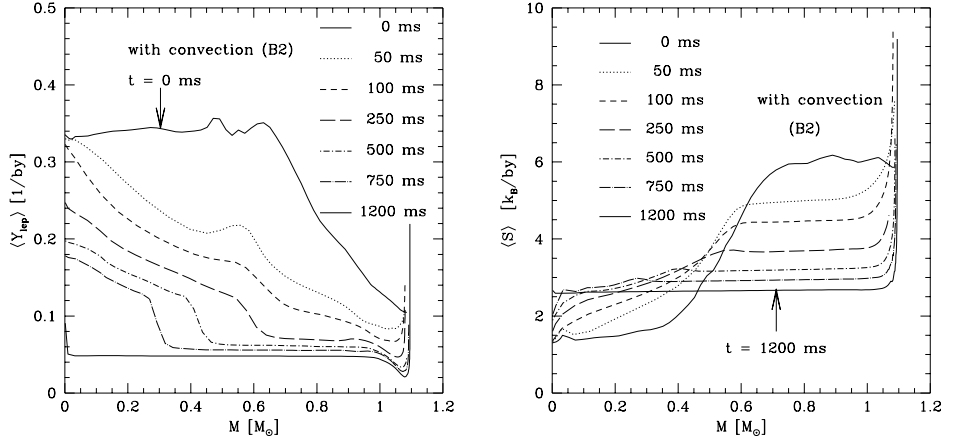

Figure 6. Same as Fig. 5, but for a two-dimensional, hydrodynamical simulation which allowed to follow the development of convection. The plots show angularly averaged quantities in the $\sim 1.1\,M_\odot$ proto-neutron star. In regions with convective activity the gradients of Y_{lep} and s are flattened. The convective layer encompasses an increasingly larger part of the star.
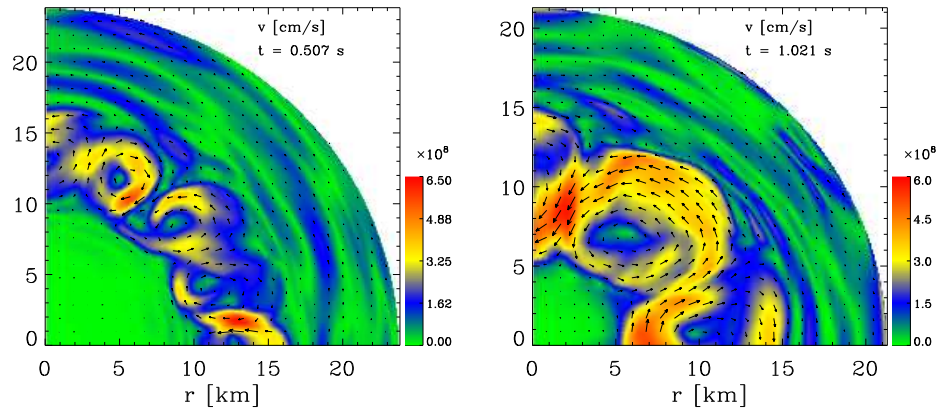
Figure 7. Absolute values of the velocity in the proto-neutron star for two instants (about 0.5 s (left) and 1 s (right) after core bounce) as obtained in a two-dimensional, hydrodynamical simulation. Note that the neutron star has shrunk from a radius of initially about 60 km to little more than 20 km. The growth of the convective region can be seen. Typical velocities of the convective motions are several 10^8 cm/s.

& Janka 1995; Sumiyoshi et al. 1995; see also Fig. 5) and have suggested the existence of regions which are potentially unstable against Ledoux convection. Recent two-dimensional, hydrodynamical simulations by Keil et al. (1996, 1997) and Keil (1997) have followed the evolution of the $\sim 1.1\,M_\odot$ proto-neutron star formed in the core collapse of a $15\,M_\odot$ star for a period of more than 1.2 seconds. These simulations have confirmed the development of convection and its importance for the evolution of the neutron star. They were performed with the hydrodynamics code *Prometheus*. A general relativistic 1D gravitational potential with Newtonian corrections for asphericities was used, $\Phi \equiv \Phi_{1D}^{GR} + (\Phi_{2D}^{N} - \Phi_{1D}^{N})$, and a flux-limited (equilibrium) neutrino diffusion scheme was applied for each angular bin separately ("$1\frac{1}{2}$D").

3.1. Phenomenology of convection in two dimensions

The simulations show that convectively unstable surface-near regions (i.e., around the neutrinosphere and below an initial density of about 10^{12} g/cm^3) exist only for a short period of a few ten milliseconds after bounce, in agreement with the findings of Bruenn & Mezzacappa (1994), Bruenn et al. (1995), and Mezzacappa et al. (1997). Due to a flat entropy profile and a negative lepton number gradient, convection, however, also starts in a layer deeper inside the star, between an enclosed mass of $0.7\,M_\odot$ and $0.9\,M_\odot$, at densities above several 10^{12} g/cm^3. From there the convective region digs into the star and reaches the center after about one second (Figs. 6 and 9). Convective velocities as high as $5 \cdot 10^8$ cm/s are found (about 10–20% of the local sound speed), corresponding to kinetic energies of up to $1–2 \cdot 10^{50}$ erg (Fig. 7). Because of these high velocities and rather flat entropy and composition profiles in the star (Fig. 6), the overshoot region is large (see Fig. 9). The same is true for undershooting during the first ~ 100 ms

11

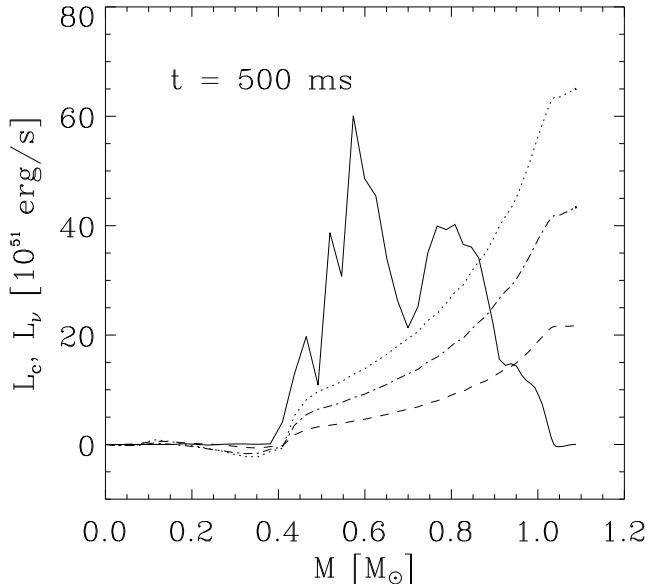Figure 8.   Convective luminosity and neutrino luminosities (dashed: $L_{\nu_e}+L_{\bar{\nu}_e}$, dash-dotted: $L_{\nu_\mu}+L_{\bar{\nu}_\mu}+L_{\nu_\tau}+L_{\bar{\nu}_\tau}$, dotted: total) as functions of enclosed baryonic mass for the two-dimensional proto-neutron star simulation at about 500 ms after core bounce.

after bounce. Sound waves and perturbations are generated in the layers above and interior to the convection zone.

The coherence lengths of convective structures are of the order of 20–40 degrees (in 2D!) (see Fig. 7) and coherence times are of the order of 10 ms which corresponds to only one or two overturns. The convective pattern is therefore very time-dependent and nonstationary. Convective motions lead to considerable variations of the composition. The lepton fraction (and thus the abundance of protons) shows relative fluctuations of several 10%. The entropy differences in rising and sinking convective bubbles are much smaller, only a few per cent, while temperature and density fluctuations are typically less than one per cent.

The energy transport in the neutron star is dominated by neutrino diffusion near the center, whereas convective transport plays the major role in a thick intermediate layer where the convective activity is strongest, and radiative transport takes over again when the neutrino mean free path becomes large near the surface of the star (Fig. 8). But even in the convective layer the convective energy flux is only a few times larger than the diffusive flux. This means that neutrino diffusion can never be neglected.

3.2.   Mechanism of convection

There is an important consequence of this latter statement. The convective activity in the neutron star cannot be described and explained as Ledoux con-
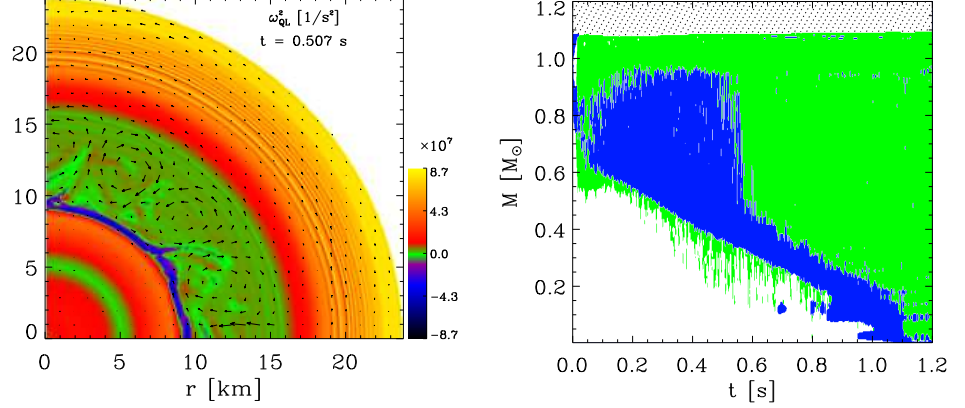
Figure 9. Left: Convectively unstable region (corresponding to negative values of the displayed quantity $\omega_{\mathrm{QL}}^2 = -(g/\rho)C_{\mathrm{QL}}$ with C_{QL} from Eq. (12)) at about 500 ms after bounce according to the Quasi-Ledoux criterion which includes non-adiabatic and lepton-transport effects by neutrino diffusion. Right: Layers of Quasi-Ledoux convective instability (blue) and gas motions with absolute velocities larger than 10^7 cm/s (green) as function of time. The criterion $C_{\mathrm{QL}}^{\mathrm{1D}}(r) \equiv \min_\theta (C_{\mathrm{QL}}(r,\theta)) > 0$ with $C_{\mathrm{QL}}(r,\theta)$ from Eq. (12) was plotted.

vection. Applying the Ledoux criterion for local instability,

$$C_{\mathrm{L}}(r,\theta) = \frac{\rho}{g}\,\sigma_{\mathrm{L}}^2 = \left(\frac{\partial\rho}{\partial s}\right)_{Y_{\mathrm{lep}},P} \frac{\mathrm{d}s}{\mathrm{d}r} + \left(\frac{\partial\rho}{\partial Y_{\mathrm{lep}}}\right)_{s,P} \frac{\mathrm{d}Y_{\mathrm{lep}}}{\mathrm{d}r} > 0 \,, \qquad (11)$$

with σ_{L} from Eq. (10) and Y_e replaced by the total lepton fraction Y_{lep} in the neutrino-opaque interior of the neutron star (for reasons of simplicity, ∇s was replaced by $\mathrm{d}s/\mathrm{d}r$ and ∇Y_{lep} by $\mathrm{d}Y_{\mathrm{lep}}/\mathrm{d}r$), one finds that the convecting region should actually be stable, despite of slightly negative entropy *and* lepton number gradients. In fact, below a critical value of the lepton fraction (e.g., $Y_{\mathrm{lep},c} = 0.148$ for $\rho = 10^{13}$ g/cm^3 and $T = 10.7$ MeV) the thermodynamical derivative $(\partial\rho/\partial Y_{\mathrm{lep}})_{s,P}$ changes sign and becomes positive because of nuclear and Coulomb forces in the high-density equation of state (see Bruenn & Dineva 1996). Therefore negative lepton number gradients should stabilize against convection in this regime. However, an idealized assumption of Ledoux convection is not fulfilled in the situations considered here: Because of neutrino diffusion, energy exchange and, in particular, lepton number exchange between convective elements and their surroundings are *not* negligible. Taking the neutrino transport effects on Y_{lep} into account in a modified "*Quasi-Ledoux criterion*",

$$C_{\mathrm{QL}}(r,\theta) \equiv \left(\frac{\partial\rho}{\partial s}\right)_{\langle Y_{\mathrm{lep}}\rangle,\langle P\rangle} \frac{\mathrm{d}\langle s\rangle}{\mathrm{d}r} + \left(\frac{\partial\rho}{\partial Y_{\mathrm{lep}}}\right)_{\langle s\rangle,\langle P\rangle} \left(\frac{\mathrm{d}\langle Y_{\mathrm{lep}}\rangle}{\mathrm{d}r} - \beta_{\mathrm{lep}}\frac{\mathrm{d}Y_{\mathrm{lep}}}{\mathrm{d}r}\right) > 0$$
$$(12)$$

(Keil 1997 and Keil et al. 1997), one determines instability exactly where the two-dimensional simulation reveals convective activity. In Eq. (12) the quantities
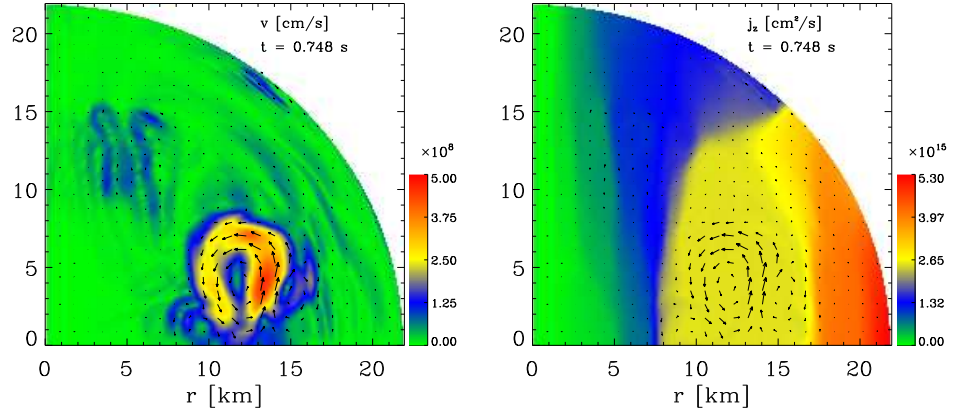
13

Figure 10. Absolute value of the gas velocity in a convecting, rotating proto-neutron star about $750\,\mathrm{ms}$ after bounce (left). Convection is suppressed near the rotation axis (vertical) and develops strongly only near the equatorial plane where a flat distribution of the specific angular momentum j_z (right) has formed.

$\langle Y_{\mathrm{lep}} \rangle$ and $\langle s \rangle$ mean averages over the polar angles θ, and local gradients have to be distinguished from gradients of angle-averaged quantities which describe the stellar background. The term $\beta_{\mathrm{lep}}(\mathrm{d}Y_{\mathrm{lep}}/\mathrm{d}r)$ with the empirically determined value $\beta_{\mathrm{lep}} \approx 1$ accounts for the change of the lepton concentration along the path of a rising fluid element due to neutrino diffusion. Figure 9 shows that at about half a second after core bounce strong driving forces for convection occur in a narrow ring between 9 and 10 km where a steep negative gradient of the lepton fraction exists (see Fig. 6). Further out, convective instability is determined only in the finger-like structures of rising, high-Y_{lep} gas.

3.3. Accretion and rotation

In very recent simulations, post-bounce mass accretion and rotation of the forming neutron star were included. Accretion leads to stronger convection with larger velocities in a more extended region. This can be explained by the steepening of lepton number and entropy gradients and the increase of the gravitational potential energy when additional matter is added onto the neutron star. Rotation has very interesting consequences, e.g., leads to a suppression of convective motions near the rotation axis because of a stabilizing stratification of the specific angular momentum (see Fig. 10), an effect which can be understood by applying the (first) Solberg-Høiland criterion for instabilities in rotating, self-gravitating bodies (Tassoul 1978):

$$C_{\mathrm{SH}}(r,\theta) \equiv \frac{1}{x^3} \frac{\mathrm{d}j_z^2}{\mathrm{d}x} + \frac{\vec{a}}{\rho} \left[\left(\frac{\partial \rho}{\partial s} \right)_{Y_{\mathrm{lep}},P} \nabla s + \left(\frac{\partial \rho}{\partial Y_{\mathrm{lep}}} \right)_{s,P} \nabla Y_{\mathrm{lep}} \right] < 0 \,. \quad (13)$$

Here, j_z is the specific angular momentum of a fluid element, which is conserved for axially symmetric configurations, x is the distance from the rotation axis, and in case of rotational equilibrium $\vec{a}$ is the sum of gravitational and centrifugal
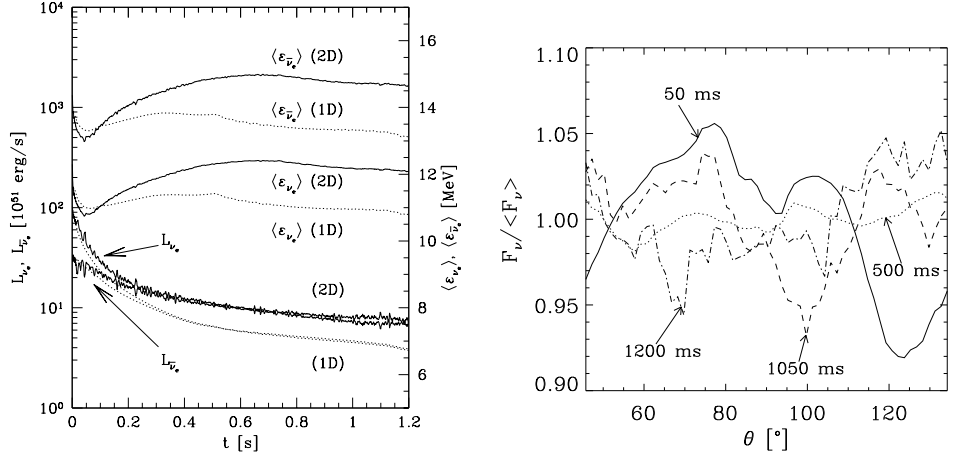
Figure 11.   Left: Luminosities $L_\nu(t)$ and mean energies $\langle \epsilon_\nu \rangle(t)$ of ν_e and $\bar{\nu}_e$ for a 1.1 $M_\odot$ proto-neutron star without ("1D"; dotted) and with convection ("2D"; solid). Right: Angular variations of the neutrino flux at different times for the 2D simulation.

accelerations, $\vec{a} = \nabla P/\rho$. Changes of the lepton number in rising or sinking convective elements due to neutrino diffusion were neglected in Eq. (13). Ledoux (or Quasi-Ledoux) convection can only develop where the first term is not too positive. In Fig. 10 fully developed convective motion is therefore constrained to a zone of nearly constant j_z close to the equatorial plane. At higher latitude the convective velocities are much smaller, and narrow, elongated convective cells aligned with cylindrical regions of $j_z = $ const parallel to the rotation axis are indicated.

The rotation pattern displayed in Fig. 10 is highly differential with a rotation period of 7.3 ms at $x = 22$ km and of 1.6 ms at $x = 0.6$ km. It has self-consistently developed under the influence of neutrino transport and convection when the neutron star had contracted from an initial radius of about 60 km (with a surface rotation period of 55 ms at the equator and a rotation period of ~ 5 ms near the center) to a final radius of approximately 22 km. Due to the differential nature of the rotation, the ratio of rotational kinetic energy to the gravitational potential energy of the star is only 0.78% in the beginning and a few per cent at the end after about 1 s of evolution.

3.4.   Consequences of proto-neutron star convection

Convection inside the proto-neutron star can raise the neutrino luminosities within a few hundred ms after core bounce (Fig. 11). In the considered collapsed core of a 15 $M_\odot$ star L_{ν_e} and $L_{\bar{\nu}_e}$ increase by up to 50% and the mean neutrino energies by about 15% at times later than 200–300 ms post bounce. This favors neutrino-driven explosions on timescales of a few hundred milliseconds after shock formation. Also, the deleptonization of the nascent neutron star is strongly accelerated, raising the ν_e luminosities relative to the $\bar{\nu}_e$ luminosities during this time. This helps to increase the electron fraction Y_e in the neutrino-heated ejecta and might solve the overproduction problem of $N = 50$ nuclei during the

15

early epochs of the explosion (Keil et al. 1996). In case of rotation, the effects of convection on the neutrino emission depend on the direction. Since strong convection occurs only close to the equatorial plane, the neutrino fluxes there are convectively enhanced while they are essentially unchanged near the poles.

Anisotropic mass motions due to convection in the neutron star lead to gravitational wave emission and anisotropic radiation of neutrinos. The angular variations of the neutrino flux determined by the 2D simulations are of the order of 5–10% (Fig. 11). With the typical size and short coherence times of the convective structures, however, the global anisotropy of the neutrino emission from the cooling proto-neutron star is certainly less than 1% (more likely only 0.1%, since in 3D the structures tend to be smaller) and kick velocities in excess of 300 km/s can definitely not be explained.

4. Conclusions

Neutrino-driven explosions are very sensitive to the structure of the progenitor star, to the details of the post-bounce dynamics, and to the properties of the neutrino emission from the nascent neutron star. Therefore type-II supernova explosions do not offer promising perspectives as standard candles.

Convective overturn in the neutrino-heated region between gain radius and supernova shock can be an important help for the explosion only if the growth timescale of the instability is shorter than the timescale for advecting accreted material through the postshock region onto the proto-neutron star. This requires a sufficiently negative entropy gradient outside the gain radius and thus strong enough neutrino energy deposition. For low neutrino luminosities this is not the case and the star does not explode. For very large neutrino luminosities the heating is so fast that the postshock layers expand and an explosion develops before convective instabilities have significantly grown. Therefore neutrino-driven convection is crucial for the explosion if one-dimensional models fail marginally, but cannot guarantee "robust" explosions independent of the size of the neutrino luminosities from the proto-neutron star.

Neutrino-driven explosions are self-regulated in the sense that the explosion energy is limited by the amount of material in the neutrino-heated region and the duration of the heating. The explosion energy is of the order of (or less than) the binding energy of the postshock layers in the gravitational potential of the proto-neutron star, because the density and thus the heated mass around the gain radius decrease drastically as soon as the explosion gains momentum and the postshock gas expands away from the neutrinosphere.

Convection inside the nascent neutron star can raise the neutrino luminosities and the mean spectral energies of the emitted neutrinos considerably and thus can be a decisive boost for the neutrino heating. In addition, proto-neutron star convection has several advantageous properties. The first two-dimensional simulations show that, on the one hand, the neutrino transport out of the interior of the star is significantly increased only after convective activity has developed in a larger part of the neutron star. In the considered collapsed core of a 15 $M_\odot$ star this requires a period of about 100–200 ms after bounce. On the other hand, since the deleptonization of the neutron star is accelerated, the electron neutrino luminosity increases relative to the antineutrino luminosity roughly between 200

and 400 ms after bounce. Both these findings may provide a remedy for the problems of current supernova models, namely to develop explosions too quickly and thus to yield rather small neutron stars and to dramatically overproduce nuclei around $N = 50$ in the ejecta (Herant et al. 1994, Burrows et al. 1995, Janka & Müller 1996). A delay of the explosion might, however, also be obtained when the restriction to two dimensions is dropped and the convective overturn turns out to be less strong in three dimensions.

The simulations performed so far can certainly not be considered as the final step. Besides the need to demonstrate the existence of convective regions in the collapsed cores of different progenitor stars, future simulations will have to clarify the influence of the nuclear equation of state on the presence of convection in nascent neutron stars. Also, a more accurate treatment of the neutrino transport in combination with a state-of-the-art description of the neutrino opacities of the nuclear medium is needed to confirm the existence of a convective episode during neutron star formation and to investigate its importance for the explosion mechanism of type-II supernovae. Three-dimensional simulations will finally be required to study the influence of the direction of the turbulent cascade (from smaller to larger structures in 2D while it is opposite in 3D) and to settle the question of hot-bubble and proto-neutron star convection quantitatively.

References

Bethe, H.A. 1990, Rev. Mod. Phys., 62, 801

Bethe, H.A. 1993, ApJ, 412, 192

Bethe, H.A., & Wilson, J.R. 1985, ApJ, 295, 14

Bruenn, S.W. 1993, in Nuclear Physics in the Universe, M.W. Guidry & M.R. Strayer, Bristol: IOP, 31

Bruenn, S.W., & Dineva, T. 1996, ApJ, 458, L71

Bruenn, S.W., & Mezzacappa, A. 1994, ApJ, 433, L45

Bruenn, S.W., Mezzacappa, A., & Dineva, T. 1995, Phys. Rep., 256, 69

Burrows, A. 1987, ApJ, 318, L57

Burrows, A., Hayes, J., & Fryxell, B.A. 1995, ApJ, 450, 830

Burrows, A., & Lattimer, J.M. 1986, ApJ, 307, 178

Herant, M., Benz, W., & Colgate, S.A. 1992, ApJ, 395, 642

Herant, M., Benz, W., Hix, W.R., Fryer, C.L., & Colgate, S.A. 1994, ApJ, 435, 339

Janka, H.-Th., & Müller, E. 1995, ApJ, 448, L109

Janka, H.-Th., & Müller, E. 1996, A&A, 306, 167

Keil, W. 1997, PhD Thesis, TU München

Keil, W., & Janka, H.-Th. 1995, A&A, 296, 145

Keil, W., Janka, H.-Th., & Müller, E. 1996, ApJ, 473, L111

Keil, W., Janka, H.-Th., & Müller, E. 1997, in preparation

Mayle, R.W., & Wilson, J.R. 1988, ApJ, 334, 909

Mezzacappa, A., Calder, A.C., Bruenn, S.W., Blondin, J.M., Guidry, M.W., Strayer, M.R., & Umar, A.S. 1997, ApJ, in press

Miller, D.S., Wilson, J.R., & Mayle, R.W. 1993, ApJ, 415, 278

Shimizu, T., Yamada, S., & Sato, K. 1994, ApJ, 432, L119

Sumiyoshi, K., Suzuki, H., & Toki, H. 1995, A&A, 303, 475

Tassoul, J.-L. 1978, Theory of Rotating Stars, Princeton: Princeton University Press, 163

Wilson, J.R., & Mayle, R.W., 1988, Phys. Rep., 163, 63

Wilson, J.R., & Mayle, R.W., 1993, Phys. Rep., 227, 97